Paper No.
13

CORROSION 98

EFFECT OF PRECORROSION ON THE PERFORMANCE OF INHIBITORS FOR CO_2 CORROSION OF CARBON STEEL

E.Gulbrandsen, S.Nesic*, A.Stangeland, T.Burchardt‡

Institute for Energy Technology

N-2007 Kjeller, Norway

B.Sundfær, S.M.Hesjevik, S.Skjerve

Statoil Research Centre

N-7005 Trondheim, Norway

ABSTRACT

Four commercially available, water soluble corrosion inhibitors for CO_2 corrosion have been tested in the laboratory on carbon steel specimens that were corroded for up to 18 days in the medium prior to inhibitor addition. The tests were performed at 20-50 °C, pH 5, 1 bar CO_2, 1-3 w% NaCl in glass cells and a glass loop. The results show that inhibitor performances were impaired with increasing precorrosion time and increasing temperature. The resulting corrosion attack was localised within deep pits. The detrimental effect is influenced both by the nature of the steel and the inhibitor composition. The inhibitor failure is related to the formation of a cementite layer at the steel surface.

Keywords: carbon dioxide, carbon steel, inhibitors, precorrosion, cementite, galvanic coupling

---

* Present address: University of Queensland, Department of Mechanical Engineering, Australia

‡ Present address: University of Oslo, Department of Chemistry, Norway

INTRODUCTION

Corrosion inhibitors for CO_2 corrosion are often tested in the laboratory using freshly ground specimens. However, in the field, the inhibitors encounter steel surfaces that are covered with different kinds of corrosion products, e.g. rust layers from pipe production, storage and testing. Furthermore, a pipeline may have been operated for several years before increasing water cut necessitate inhibition. In this case the metal surface might be covered with iron carbonate precipitates, uncorroded iron carbide, and different types of scale. These products may significantly affect the performance of the inhibitor. The problem of precorrosion is thus relevant to oil field applications of inhibitors. In the present work the results of inhibitor tests with up to 18 days precorrosion are shown. These tests were part of a larger inhibitor testing programme carried out by Statoil and Institute for Energy Technology (IFE).

Little work has yet been devoted to corrosion inhibition at steel surfaces covered with corrosion product layers. Kowata[1] reviewed the work done on rusted surfaces, and showed that some inhibitors are able to penetrate deep into the rust layer. Hausler[2] considered inhibition of CO_2 corrosion under conditions where $FeCO_3$ films predominated. The concept of interphase inhibition has been developed[3-4] to describe inhibition in (and by) porous corrosion product layers (as opposed to interface inhibition at bare surfaces[3]). Kapusta et al.[5] found that 1 day precorrosion had a negative effect on the inhibitor performance. Hausler and co-workers[6-7] concluded that 4 days precorrosion did not significantly affect the inhibitor performance in tests at high CO_2 partial pressure and high temperature. Dougherthy and Stegman[8] found that certain oil soluble inhibitors actually performed better on precorroded surfaces. A preliminary account of the present study has been published elsewhere[9]. From this brief overview of the existing knowledge on how precorrosion affects inhibition, it is clear that more work is needed to clarify the effects.

EXPERIMENTAL

Six different commercially available inhibitors from three different suppliers were tested in the programme. In the present study the focus will be placed on the four inhibitors (Table 1) which were most extensively tested with respect to precorrosion. The inhibitors were tested on a number of different steels. We report results on three different steels, here denoted X65, 0.5% Cr and St52 in shorthand notation. The element analyses, microstructures and complete designations of these steels are given in Table 2. St52 is a typical construction steel, while X65 and 0.5% Cr are both being used as pipeline materials.

The inhibitor tests were performed at 20-50 °C, pH 5, 1 bar CO_2, and 1-3 w% NaCl under natural convection conditions in glass cells and under straight pipe flow conditions in a glass corrosion loop. Test solutions were made up from distilled water (glass cell experiments) or reverse osmosis water (loop experiments) and puriss (>99.9%) NaCl. The electrolytes were deoxygenated and CO_2 saturated by bubbling CO_2 gas (>99.98%) at 1 bar pressure. The solution pH was adjusted with HCl or $NaHCO_3$. The details of the experimental conditions are given in the figure captions. Prior to immersion the specimens were pre-treated by grinding to 1000 grit with SiC paper, degreasing in acetone, and flushing in ethanol.

The corrosion rates were determined electrochemically by linear polarisation resistance (LPR)

measurements in three-electrode configuration. Slow potentiodynamic polarisation sweep measurements were performed to obtain additional information about the corrosion process. All the reported results have been corrected for uncompensated solution resistance determined by electrochemical impedance measurements. Mass loss measurements[10] were performed on selected specimens to verify the LPR data. The parameters used for the electrochemical measurements and corrosion rate calculations are summarised in Table 3.

Cylindrical specimens were used in the glass cells, Fig. 1. The cylinders were mounted on PTFE coated steel rods. The counter electrode was a ring shaped platinum wire placed inside the cell, surrounding the specimen. The Ag/AgCl reference electrode was located in a separate compartment, being connected to the cell by means of a wooden plug salt bridge and a Luggin capillary. The glass cells were filled with 3 litres of electrolyte. The Fe^{2+} content in the electrolyte was determined regularly by chemical analysis. The electrolyte was replenished at regular intervals during long time experiments in order to keep the iron content below saturation of $FeCO_3$. The saturation concentration of Fe^{2+} is[11] 240 ppm at 20 °C and 85 ppm at 50 °C (pH 5, 1 bar CO_2). The iron content was held below 20 ppm.

Specimens mounted flush with the pipe wall were used in the IFE glass loop, Fig. 2. The tubular specimen holder had an internal diameter of 15 mm. A diametrically mounted specimen of a corrosion resistant alloy was used as the counter electrode. The reference electrode was connected to the electrolyte through a 5 mm wooden plug salt bridge adjacent to the specimen. The loop was filled with 150-200 litres of electrolyte. Also in these experiments, the electrolyte was replenished to maintain a low Fe^{2+} concentration (below 30 ppm). The content of dissolved O_2 in the solution was continuously monitored with an O_2 detector. The concentration was normally below 10 ppb, but ocassionally reached 100-200 ppb during insertion of specimens. A more detailed description of the loop is given elsewhere[12].

RESULTS AND DISCUSSION

The tests were conducted under conditions where the uncorroded cementite from the steel itself constitutes the dominant part of the corrosion product film. The iron content was kept low in order to avoid precipitation of iron carbonate at the steel surface.

Glass cell tests of Inhibitor A.

The effect of the imidazoline based Inhibitor A concentration was initially tested on freshly ground specimens without any precorrosion. The results, Fig. 3, shows that final corrosion rates below 0.1 mm/y were obtained with 20 ppm of the inhibitor, corresponding to an inhibitor efficiency of about 95 %. At very high concentrations (200 ppm) pitting corrosion was initiated. The recommended dosage for this inhibitor is 20-50 ppm. However, the tests with precorrosion indicated that this recommended concentrations may be too low. The effect of precorrosion time is illustrated by the results of a test of the same inhibitor on X65 and St52 steels shown in Fig. 4. Three important trends are evident. Firstly, for both steels the corrosion rate increased during the precorrosion period. Secondly, the inhibitor efficiency decreased with increasing precorrosion time. And, thirdly, this decrease in inhibitor efficiency is much larger for St52 than for X65 steel. On X65 specimens (Fig. 4a)

Inhibitor A (20 ppm) worked efficiently even after 14 days precorrosion, giving a final corrosion rate of about 0.1 mm/y. It was noted, however, that the inhibitor acted slower with increasing precorrosion time. On St52 specimens (Fig. 4b) the inhibitor performed acceptably after 3 days precorrosion, but with longer precorrosion times the inhibition kinetics apparently became much slower. The specimens that were precorroded 10 and 14 days were practically not protected at all by the inhibitor. Obviously, the effect of precorrosion is influenced by the properties of the steel.

The noted increase in corrosion rate during the precorrosion period has previously been attributed to several factors: (1) removal of a protective oxide film[5], (2) galvanic coupling to the uncorroded iron carbide (cementite) film[5], (3) increase in the true specimen surface area[5], and (4) acidification of the solution inside the corrosion product film[13]. As the inhibition problems seen above may be related to one or more of these phenomena, some discussion on this subject is needed.

Figure 5 shows so-called pseudo-polarisation curves[13] for some of the experiments reported in Fig. 4a-b. The pseudo-polarisation curves show how the corrosion point (E_{cor}, I_{cor}) moves with time in a Tafel plot during the eperiment. Also shown is the potentiodynamic polarisation curves for a freshly ground electrode exposed in a parallel test under the same conditions. Pseudo-polarisation curves essentially gives information on whether the free corrosion point, during a process of change at the specimen, follows the the anodic or cathodic polarisation curves. In Fig. 5, the corrosion point follows more or less the anodic polarisation curve for the freshly ground specimen, indicating that the anodic Tafel curve is little affected during the precorrosion period, whereas the cathodic curve is shifted to higher rates (see also Fig. 8). The slopes of the anodic curves and the pseudo-polarisation curves are 0.05 V/decade for X65 specimens and 0.06 V/decade for St52. The behaviour observed here is indicative of a galvanic effect of the cementite layer[13], where the surface area of the cathodic cementite particles increases with time. After inhibitor addition, the corrosion potential of X65 increased sharply for the first few hours (Fig. 5a) without a drop in corrosion rate. This indicates mainly an anodic inhibition in this period, the corrosion rate being determined by the reaction limited cathodic current[14]. With time the cathodic reaction is also inhibited, and the corrosion point follows approximately the inhibited anodic curve. For St52 steel the same processes do occur at the specimen precorroded 3 days (Fig. 5b), but not on the specimen precorroded 14 days.

Figure 6 shows scanning electron microscopy (SEM) micrographs of cross sections of the specimens precorroded 14 days in Fig. 4a-b. The images show that the St52 steel specimen had a very pronounced cementite film, whereas little cementite film could be seen on the X65 specimen. The main reason for this is that the carbon content of the St52 steel is much higher, Table 2. Furthermore, the cementite particles on X65 did not seem to form a network like on the St52 steel. The SEM images show that no significant precipitation of other phases, such as the iron carbonate had taken place.

These SEM observations points to one important difference between X65 and St52 steels, namely the size and morphology of the cementite layer. This difference could explain the large variation in inhibitor performance on precorroded specimens. It was therefor decided to perform some experiments that focused specifically at the role of the cementite layer. In the first experiment a cementite film was grown on X65 and St52 specimens during 7-9 days precorrosion at room temperature, Fig. 7. A rise in the corrosion rate was observed during this period, similar to the results in Fig. 4. After 7-9 days the cementite layer was removed from the specimen surface with a test tube brush (without removing the specimen from the solution). The corrosion rate and the corrosion

potential immediately reverted to the values they had at the start of the experiment. 20 ppm of Inhibitor A was added to the St52 specimen ca. 6 h later; the inhibitor worked slower than on a bare surface, but it did work and the final corrosion rate dropped to 0.1 mm/y. The inhibitor thus performed better on this specimen than on the comparable specimens precorroded 3 or 7 days in Fig. 4b. Figure 8 illustrates how the electrochemical reactions were affected by the growth and removal of the cementite film on St52. Polarisation curves measured at start, after 7 days precorrosion (with film) and after film removal are plotted together with the pseudo-polarisation curve for the precorrosion period. The anodic curves (Tafel slope ca. 35 mV/decade) nearly overlap for the three cases, showing that the anodic dissolution was little affected. The change in the true anodic surface area of the specimen is thus rather small. The pseudo-polarisation curve follows closely the anodic curves. The cathodic rate increased strongly during the precorrosion, which may be interpreted as an increase in the area of the cathodic cementite particles, see Appendix A. When the film was removed, the cathodic curve reverted to about the same position as at the start of the test.

A few tests were performed on a pure (>99.998%) iron specimen. The results displayed in Fig. 9 show that the corrosion rate was nearly constant during the precorrosion period. The corrosion potential was also constant at about –0.705 V. The inhibitor worked fast and efficiently. No corrosion products could be seen at the specimen by optical microscopy.

Summarising the results presented above, it can be concluded that the increase in corrosion rate observed during precorrosion is caused by the growing cementite film. No such increase was observed on pure iron, and the increase was less pronounced on X65 (low carbon) than on St52 (high carbon). The corrosion rate on St52 dropped immediately when the cementite film was removed. The corrosion rate increase is thus probably caused by the galvanic effect of the cathodic cementite, confer Fig. 5, Fig. 8 and Appendix A. Explanations based on removal of a possible oxide film, increasing anodic area or acidification do not seem to be fully consistent with the experimental results.

The results also indicate that the inhibitor failure following long time precorrosion is related to the presence of a cementite film. The inhibitor worked efficiently when little or no cementite film was present, i.e. on pure iron, on freshly ground steel specimens, on X65 steel (as compared to St52), and when the film was removed. On the contrary, the inhibitor showed impaired efficiency with increasing thickness of the cementite layers (St52 in particular, but also to some extent X65, see also below). However, other factors may contribute to the impaired inhibitor efficiency. This aspect will be discussed briefly after the presentation of the results of the glass loop tests.

Glass loop tests of Inhibitors B, C and D

Inhibitor B and Inhibitor C were tested in the glass loop at 20 °C, pH 5, 1 bar CO_2 and 1 m/s flow velocity. The results are shown in Fig. 10a-b. In these experiment, also a 0.5% Cr specimen was included. The specimens were precorroded for 15 days. The corrosion rate increased continuously for X65 and St52, but for 0.5% Cr the increase was small. Addition of 25 ppm of the imidazoline based Inhibitor B had little effect on the St52 specimen, whereas it provided better inhibition for the X65 (74% efficiency) and 0.5% Cr (94% efficiency) specimens, Fig. 10a. Improved inhibition was achieved for all specimens, except St52, by raising the inhibitor concentration to 55 ppm after 18 days. Inhibitor C, which was amine based, performed significantly better at 25 ppm (Fig. 10b). Even St52 obtained some protection. The relative ranking between the different steels with

respect to corrosion rate and inhibitor efficiency was however the same as with Inhibitor B.

The precorrosion effect became more severe when the temperature was increased. Inhibitor C and Inhibitor D were tested at 50 °C, pH 5 and 1 m/s flow velocity. The specimens were precorroded for 18 days, and the experiment was continued 40-50 days after inhibitor addition. The results are reported in Fig. 11a-b. Inhibitor C performed slightly better than Inhibitor D, but none of the specimens obtained stable corrosion rates below 1 mm/y. Freshly ground specimens were also inserted during this period. The inhibitors worked efficiently on these specimens, showing that thermal or chemical breakdown of the inhibitors could not explain the poor efficiency on the precorroded specimens. In the test of Inhibitor D the X65 specimen was taken out of the solution after 60 days (see arrow in Fig. 11b), and the corrosion products were removed by careful brushing before the specimen was reinserted. The corrosion rate decreased by more than half a decade. In a similar manner, the corrosion product film on the 0.5% Cr specimen was removed after 48 days in the test of Inhibitor C (Fig. 11a). The effect of this treatment was small.

Examination of the exposed specimens following the experiment with Inhibitor C revealed localised attack of X65 and 0.5% Cr steel, Fig. 12. Parts of the X65 specimen surface were protected, but at certain spots the corrosion continued at high rates, giving deep spherical pits (Fig. 12 a). Parts of the cementite film are visible in the cross section. After 18 days precorrosion at 5-10 mm/y, the cementite layer was quite pronounced also at X65 steel, Fig. 12 b. Smaller and more open pits were observed at 0.5% Cr (Fig. 12 c), whereas at St52 no parts of the surface were protected and the attack was nearly uniform (Fig. 12 d). The largest pit seen in Fig. 12 a has a diameter of about 0.6 mm, indicating a corrosion rate of 3 mm/y or more inside it during the 40 days period after inhibitor addition.

The loop test results show that impaired inhibitor performance after long time precorrosion may be a rather general problem with inhibitors for CO_2 corrosion. The inhibition problems observed in these tests seem to be related to the presence of a cementite layer at the steel surface. The thicker the cementite film grows, the more severely the inhibitor performance is impaired. This can best be seen by the results in Fig. 11. The specimens corroded at high rates during 18 days. causing poor inhibitor performance for both inhibitors on all the tested steels.

The SEM micrographs in Fig. 12 provides interesting information about the nature of the corrosion attack at precorroded specimens in the presence of inhibitor. The long exposure time after inhibitor addition facilitated the observation of the localised attack connected to the inhibitor failure. The surface appears to be protected in certain regions. The corrosion continued at high rates in other locations, giving rise to spherical pits. The galvanic effect of the cementite film may contribute to maintain a high corrosion rate inside the pits. This may be why the corrosion rate dropped when the X65 specimen was taken out and brushed, Fig. 11b. The localised attack seen on X65 was typical for 5 other steels actually tested in this experiment. There also seemed to be a certain correlation (inverse) between apparent inhibitor efficiency and the number of pits. That is, the apparent inhibitor efficiency is calculated from average corrosion rates. Accordingly, the higher the number of pits, the higher the average corrosion rate, and the lower the apparent inhibitor efficiency.

The thick cementite layers will certainly form a transport barrier for the inhibitor compounds. However, the fact that the specimens are not protected even after 40-50 days with inhibitor present and

1 m/s flow, indicate that this is not only a question of transport problems for the inhibitor. An inhibited carbon steel surface is in a very unstable condition, just like for a passivated metal. The driving force for corrosion is large, but corrosion is kinetically hindered. A large cathodic surface contributes to make the condition more unstable and thus promote pitting at weak spots in the inhibitor film. Such weak spots may arise due to defects in the steel surface (grain boundaries, inclusions etc.) or by low inhibitor concentrations locally in the cementite film. Furthermore, high metal dissolution rates locally may prevent slowly adsorbing inhibitors from adsorbing. This phenomenon is described by the electromechanical inhibitor desorption model of Drazic et al[15], where it is assumed that inhibitor molecules are desorbed when the substrate metal atom goes into solution. For example, at 5 mm/y about 1 monolayer of iron is dissolved per second. In combination with low inhibitor concentration locally, this effect may become critical.

Some of the results obtained in the inhibitor tests gave reason to suspect that certain alloying elements also contribute to the observed inhibition problems. This complex issue is presently under investigation at IFE . However, no firm knowledge has yet been obtained. A few tests carried out with other types of corrosion product films indicated that rust layers and carbonate layers did not affect inhibitor performance in a negative way compared to the ground specimens, again suggesting that the film does not affect the inhibitor performance soleley by reducing the diffusion rate.

The present test results point out a phenomenon that may contribute to failure of inhibitors in field applications. It was, however, demonstrated that there were significant differences in the performance between different inhibitors on precorroded specimens. It was also shown that the typical pipeline steels with low carbon content was better protected than the construction steel. It thus appears that these precorrosion effects may be overcome through proper inhibitor testing and selection. Precorrosion effects should therefor be given more attention in inhibitor testing.

CONCLUSION

Four commercial inhibitors for CO_2 corrosion have been tested in glass cells and in a glass corrosion loop on carbon steel specimens that were corroded up to 18 days prior to inhibitor addition. The precorrosion and test conditions were: 20-50 °C, pH 5, 1 bar CO_2 and 1-3 w% NaCl. Under these precorrosion conditions mainly cementite corrosion films were formed. Based on the test results, the following conclusions can be drawn:

- Inhibitor performances were in general impaired after long time precorrosion under the given conditions.
- The poor inhibition resulted in localised corrosion attacks with deep spherical pits.
- The detrimental effect of precorrosion is co-determined by the steel properties and the inhibitor compositions. The precorrosion effect seems to be related to the presence of a cementite layer at the steel surface.
- The results show that the problem probably can be overcome by careful selection of inhibitors. The effect of long time precorrosion should be given more attention when inhibitors are tested. The steels tested should be representative for the pipeline steel to be protected.

- 0.5% Cr steel generally obtained better protection than X65 steel without Cr.

ACKNOWLEDGEMENT

This work was financed by Statoil and IFE. The authors appreciate the permission granted by Statoil to publish these results.

REFERENCES

1. K.Kowata and K.Takahashi, "Interaction of Corrosion Inhibitors with Corroded Steel Surface", CORROSION 96, paper no. 219, (Houston, TX: NACE International, 1996).

2. R.H.Hausler, "Corrosion Inhibition in the presence of Corrosion Product Layers", Proc. 6th European Symposium on Corrosion Inhibitors (6SEIC): Ann. Univ. Ferrara, N.S., Sez. V, Suppl. N. 8, 1985 (Ferrara, 1985), p. 41.

3. K.Juttner, W.J.Lorenz and F.Mansfeld, "Interface and Interphase Inhibition", CORROSION 89, paper no. 135, (Houston, TX: NACE International, 1989).

4. M.Mitzlaff, W.Ritschel, H.Wirtz, D.Miller, H.N.Hoffmann, H-H.Strehblow and W.J.Lorenz, Werkstoffe und Korrosion 40 (1989), p. 629.

5. S.D.Kapusta, P.R.Rhodes and S.A.Silverman, "Inhibitor Testing for CO_2 Environments", CORROSION 91, paper no. 471, (Houston, TX: NACE International, 1991).

6. R.H.Hausler, D.W.Stegman, C.I.Cruz and D.Tjandroso, "Laboratory Studies on Flow Induced Localized Corrosion in CO_2 / H_2S Environments. III. Chemical Corrosion Inhibition", CORROSION 90, paper no. 7, (Houston, TX: NACE International, 1990).

7. R.H.Hausler and D.W.Stegman, "Laboratory Studies on Flow Induced Localized Corrosion in CO_2 / H_2S Environments. IV. Assessment of the Kinetics of Corrosion Inhibition by Hydrogen Evolution Measurements", CORROSION 91, paper no. 474, (Houston, TX: NACE International, 1991).

8. J.A.Dougherty and D.W.Stegmann, "The Effects of Flow on Corrosion Inhibitor Performance", CORROSION 95, paper no. 113, (Houston, TX: NACE International, 1995) and Materials Performance 35, 4(1996): p. 47.

9. E.Gulbrandsen, B.Sundfær, S.M.Hesjevik, S.Skjerve, S.Nesic and T.Burchardt, "Effect of Precorrosion on the Performance of Inhibitors for CO_2 Corrosion of Carbon Steel", Proc. EUROCORR '97 (Trondheim: European Federation of Corrosion, 1997), p. 183.

10. P. Fazio et al.(Editors), ASTM Standard Practice G 1 - 90, "Standard Practice for Preparing, Cleaning, and Evaluating Corrosion Test Specimens", Annual Book of ASTM Standards Vol. 03.02, (Philadelphia, PA: American Society for Testing and Materials, 1992), pp. 35-41.

11. In-house computer program for solubility calculations. Version 2.0, Institute for Energy Technology (1997).

12 S.Nesic, G.Solvi, and J.Enerhaug, "Comparison of the Rotating Cylinder and Pipe Flow Test for Flow Sensitive CO_2 Corrosion", CORROSION 95, paper no. 130, (Houston, TX: NACE International, 1995).

13. J-L.Crolet, S.Olsen and W.Wilhelmsen, "Influence of a Layer of Undissolved Cementite on the Rate of the CO_2 Corrosion of Carbon Steel", CORROSION 94, paper no. 4, (Houston, TX: NACE International, 1994).

14. S.Nesic, J.Postlethwaite and S.Olsen, "An Electrochemical Model for Prediction of CO_2 Corrosion", CORROSION 95, paper no. 131, (Houston, TX: NACE International, 1995).

15. V.J.Drazic and D.M.Drazic, "Influence of the Metal Dissolution Rate on the Anion and Inhibitor Adsorption", Proc. 7th European Symposium on Corrosion Inhibitors (7SEIC): Ann. Univ. Ferrara, N.S., Sez. V, Suppl. N. 9, 1990 (Ferrara, 1990), p. 99.

TABLE 1

INHIBITORS FOR CO_2 CORROSION TESTED FOR PRECORROSION EFFECT. ALL INHIBITORS WERE WATER SOLUBLE.

Inhibitor	Active compound
A	Imidazoline
B	Imidazoline
C	Amine
D	Amine

TABLE 2

DESIGNATIONS AND ELEMENT ANALYSIS (W%) FOR THE CARBON STEELS USED IN THE INHIBITOR TESTS

Steel		Designation	Microstructure
X65	(#56)*	API 5L X65	Ferrite-perlite
0,5% Cr	(#50)*	API 5L X65	Ferrite-Wiedmanstätten
St52	(#53)*	St. 52-3	Ferrite-perlite

* Internal IFE steel reference number.

Steel	C	Si	Mn	S	P	Cr	Ni	V	Mo	Cu	Al	Sn	Nb
X65	0,064	0,26	1,55	0,001	0,012	0,05	0,04	0,035	0,01	0,04	0,041	0,002	0,041
0,5%Cr	0,072	0,17	0,89	0,002	0,014	0,6	0,02		0,01	0,01	0,038	0,001	
St52	0,13	0,38	1,29	0,008	0,015	0,07	0,09	0,035	0,01	0,34	0,05	0,015	

TABLE 3

PARAMETERS FOR ELECTROCHEMICAL CORROSIONS MEASUREMENTS

Test specimens -glass cell: cylinder	10 mm ∅ x 10 mm H, S=3.14 cm^2
-loop: pipe wall flush	S=2.9 cm^2
Linear Polarisation Resistance (LPR) - R_p	Potential ramp -5 to +5 mV *vs* E_{cor}
- sweep rate	0.1 mV/s
Potentiodynamic Sweep - cathodic	Potential ramp 0 to -600 mV *vs* E_{cor}
- anodic	0 to +150 mV *vs* E_{cor}
- sweep rate	0.2 mV/s
Electrochemical Impedance Spectroscopy (EIS)	± 5 mV rms., 5 kHz - 0.1 Hz
Corrosion Current Density, I_{cor}	I_{cor} = B/(R_p S) , B = 17-20 mV *
Corrosion Rate, v_{cor}	v_{cor}(mm/y) = 1.16 I_{cor}(A.m^{-2})
Reference Electrode	Ag/AgCl (3 M KCl) E= 0.194 V *vs. she*

* B value based on mass loss data

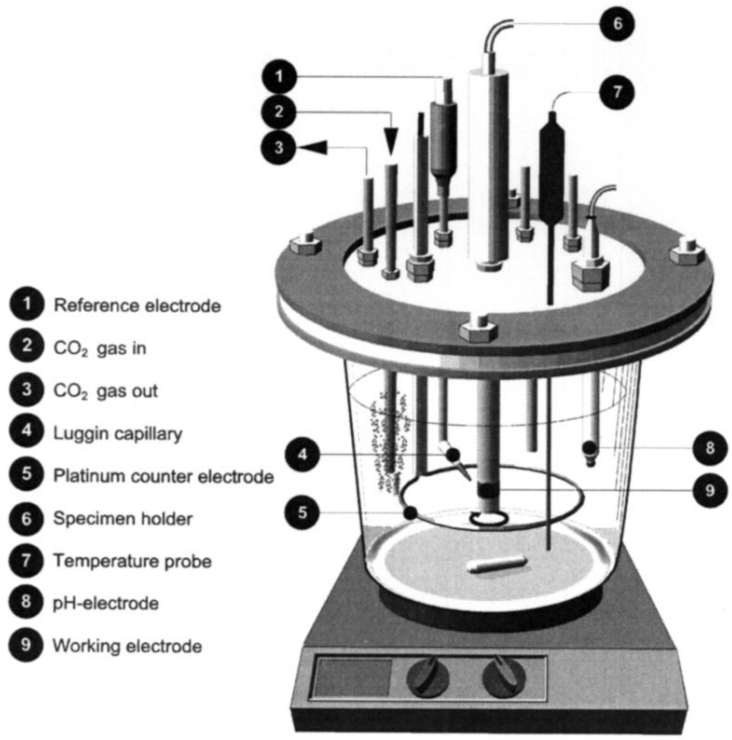

FIGURE 1. Glass cells used for inhibitor tests.

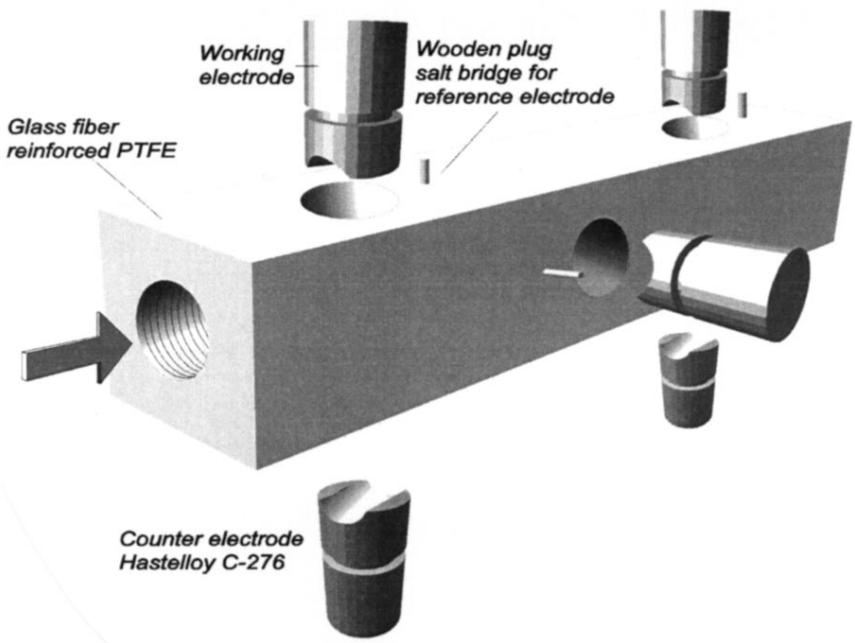

FIGURE 2. Specimen holder for straight pipe flow geometry in the glass loop.

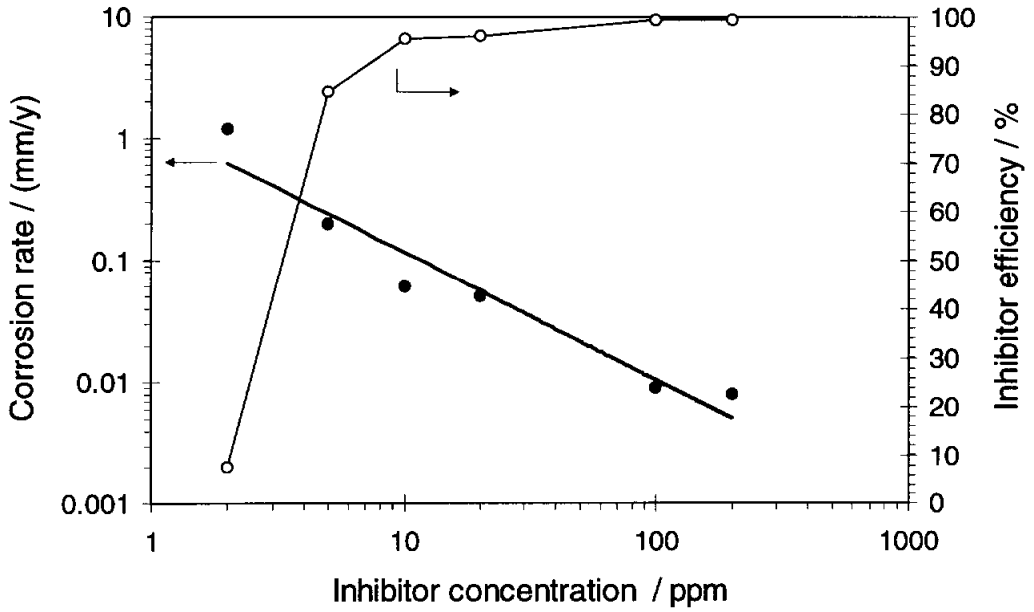

FIGURE 3. Corrosion rate and inhibitor efficiency of freshly ground X65 specimen vs. concentration of the imidazoline based Inhibitor A. The corrosion rates was read after 24 h inhibition. Experimental conditions: 20 °C, pH 5, 1 bar CO_2 , 1 % NaCl, natural convection.

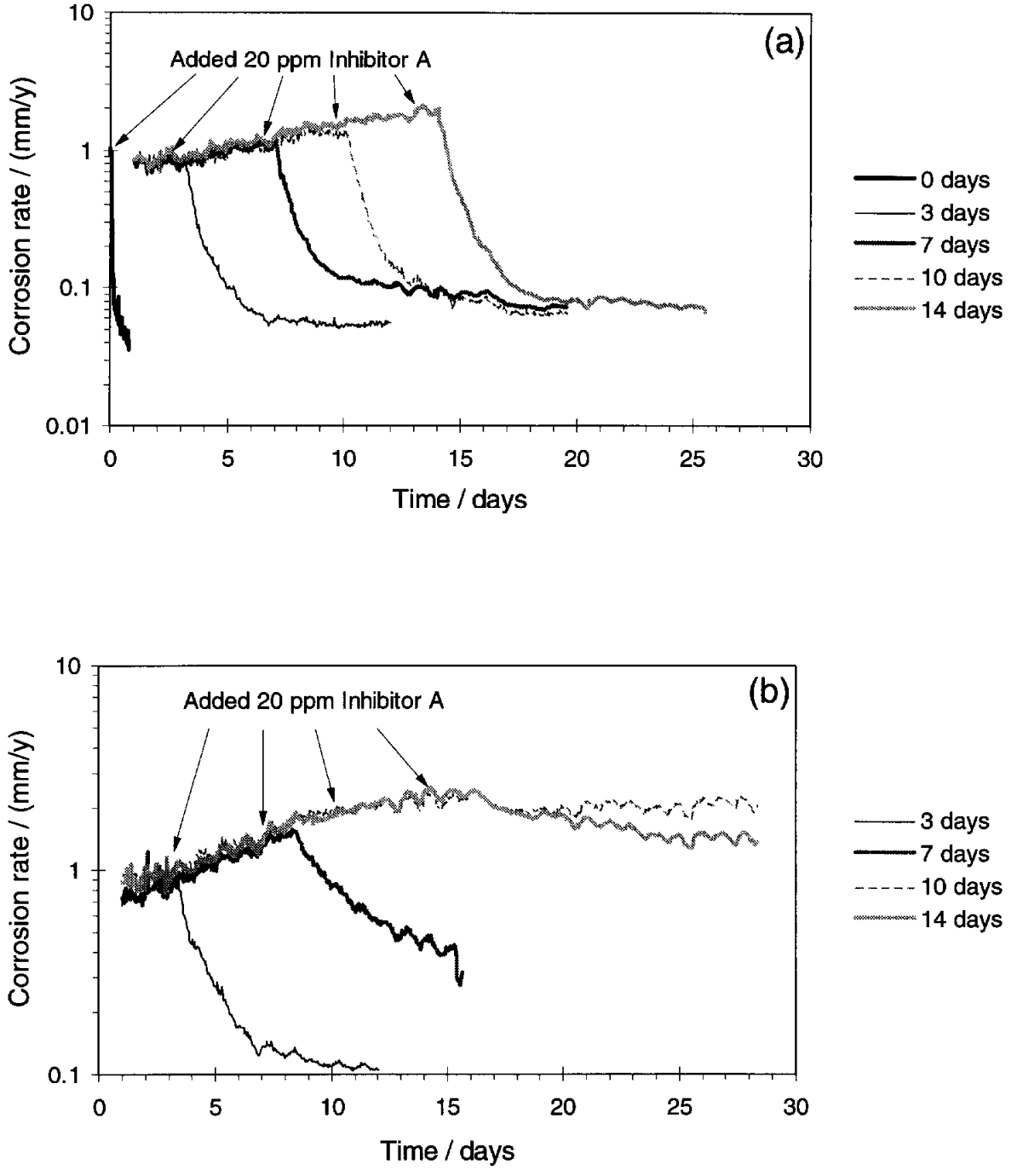

FIGURE 4. Average corrosion rate of (a) X65 specimens and (b) St52 specimens vs. time in experiments with the imidazoline based Inhibitor *A*. The precorrosion times are given in the legends, and the arrows show the points of time when inhibitor was added to the different glass cells. Experimental conditions: 20 °C, pH 5, 1 bar CO_2, 1 % NaCl, natural convection.

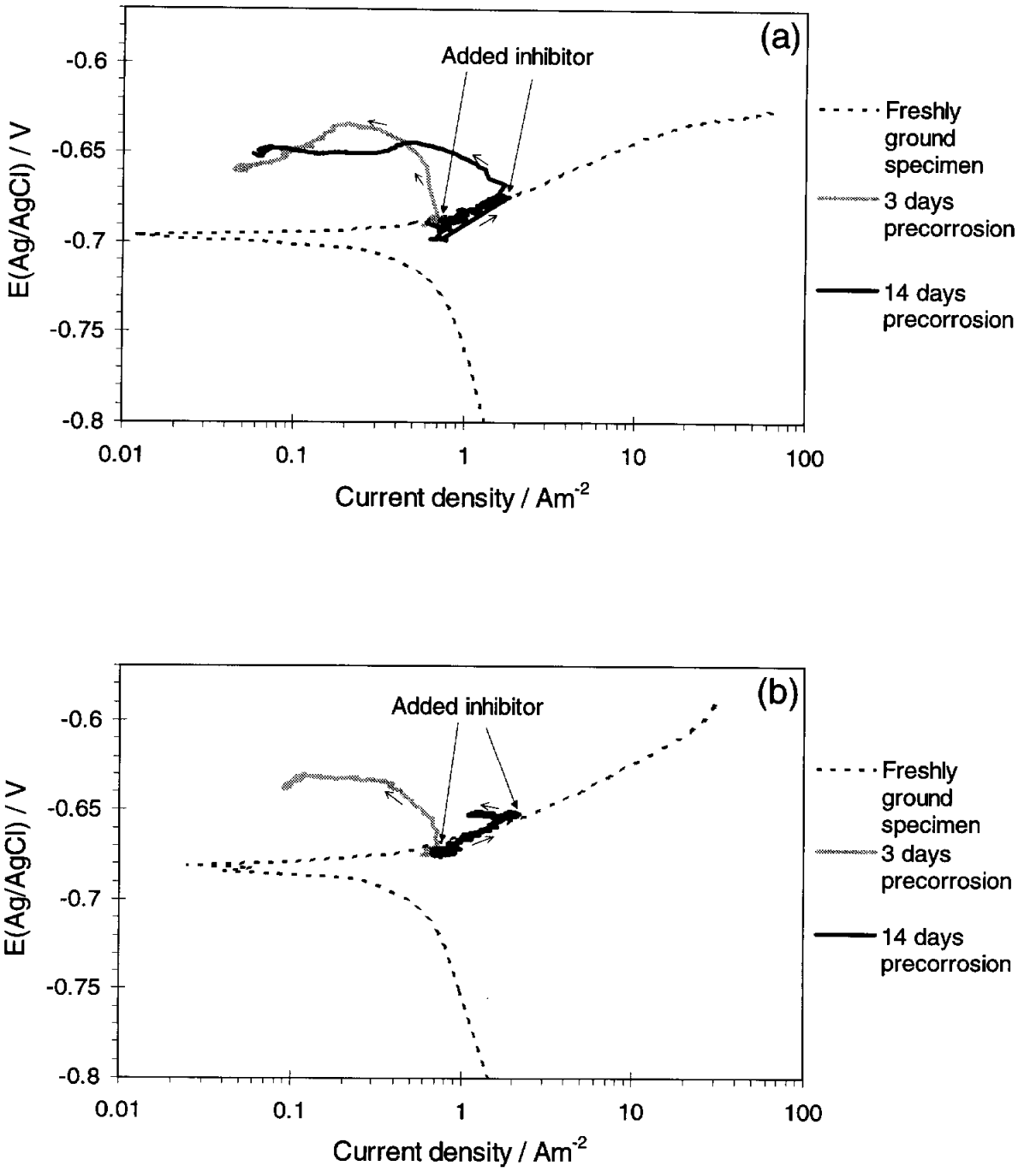

FIGURE 5. Pseudo-polarisation curves for the experiments with the imidazoline based Inhibitor A in Fig. 4a-b. (a) X65 and (b) St52. The thin dashed curves are polarisation curves measured on freshly ground specimens of the respective steels. Experimental conditions: 20 °C, pH 5, 1 bar CO_2, 1 % NaCl, natural convection.

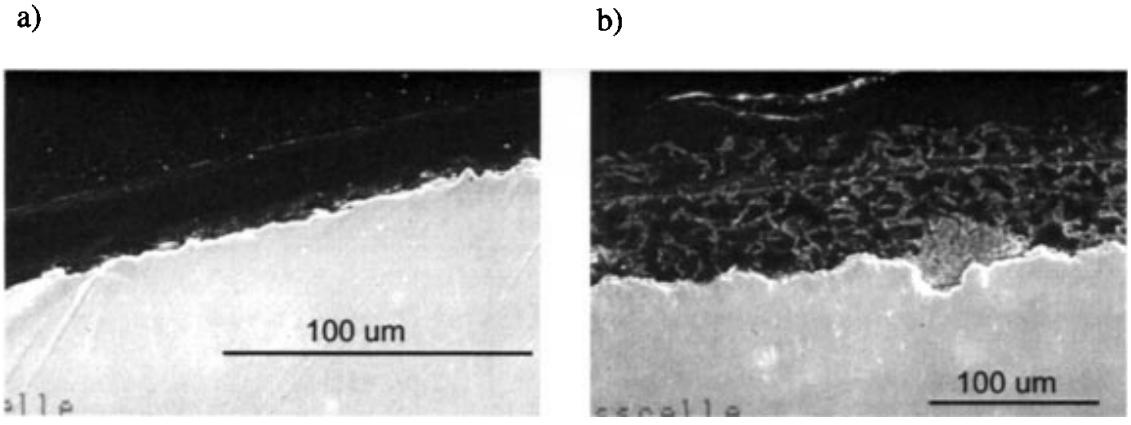

FIGURE 6. Scanning electron micrographs of specimens exposed in the experiments with the imidazoline based Inhibitor A in Fig. 4a-b. Cross sections of (a) X65 and (b) St52 specimen, both precorroded 14 days. Experimental conditions: 20 °C, pH 5, 1 bar CO_2, 1 % NaCl, natural convection.

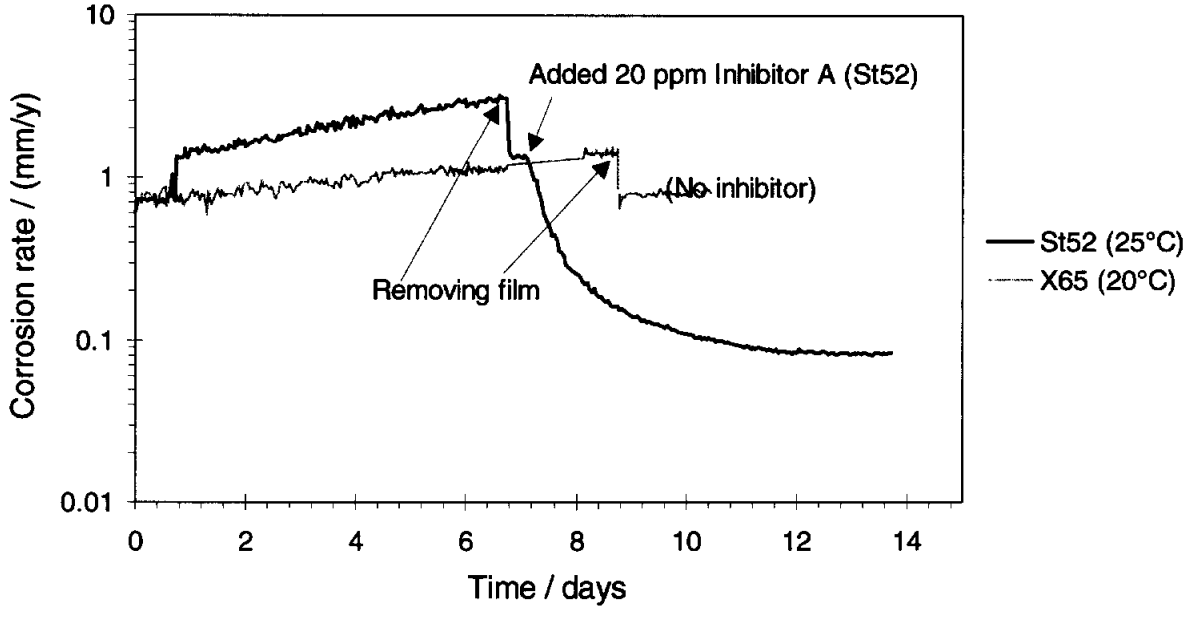

FIGURE 7. Average corrosion rate vs. time in experiments where the layer of uncorroded cementite was removed. The arrows show the points of time when the film was removed and inhibitor added (20 ppm imidazoline based Inhibitor A). Experimental conditions: 20-25 °C, pH 5, 1 bar CO_2, 1 % NaCl, natural convection.

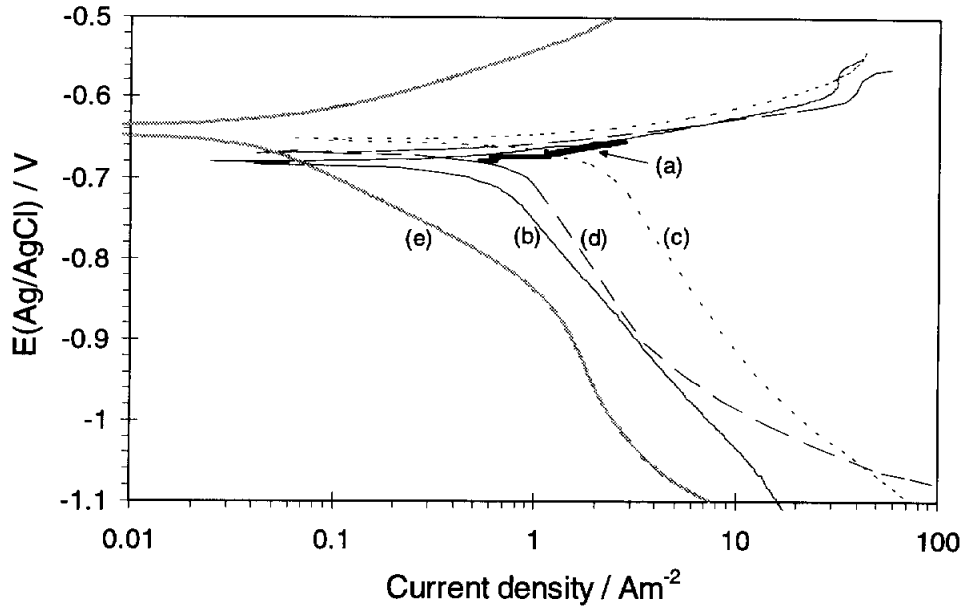

FIGURE 8. Polarisation curves for the experiments with cementite film removal on St52 specimens in Fig. 7. The thick Curve (a) shows the pseudo-polarisation curve for the time up to inhibitor addition. The thin curves represent potentiodynamic polarisation curves, where Curve (b) was measured at a freshly ground specimen, Curve (c) after 7 days precorrosion with the cementite film intact, and Curve (d) after removal of the film. Curve (e) is the polarisation curve after inhibition with 20 ppm imidazoline based Inhibitor A. Experimental conditions: 25 °C, pH 5, 1 bar CO_2, 3 % NaCl, natural convection.

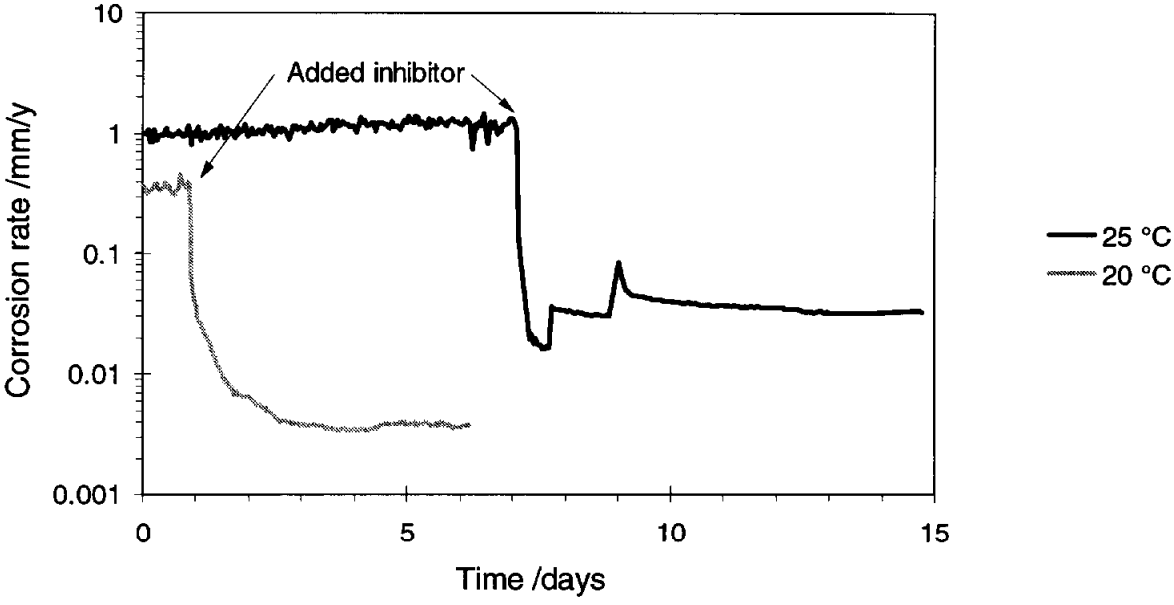

FIGURE 9. Corrosion rate vs. time for pure iron (>99.998%) specimen under precorrosion and inhibition. 20 ppm imidazoline based Inhibitor A was added after 1 and 7 days precorrosion. Experimental conditions: 20-25 °C, pH 5, 1 bar CO_2, 1-3 % NaCl, natural convection.

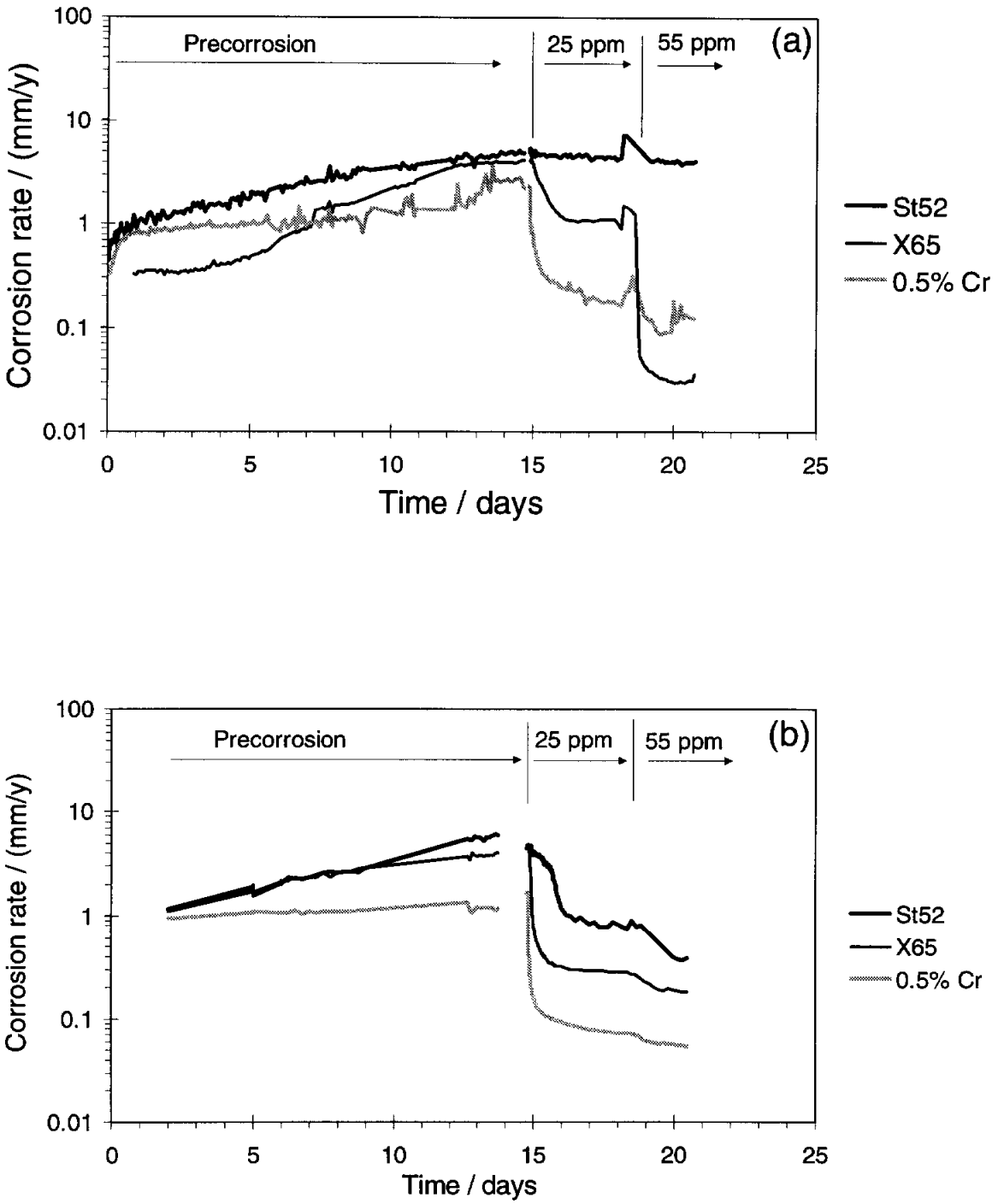

FIGURE 10. Average corrosion rate vs. time in loop experiments with (a) Inhibitor B (imidazoline based) and (b) Inhibitor C (amine based). Experimental conditions: 20 °C, pH 5, 1 bar CO_2 , 1 % NaCl, pipe flow 1 m/s.

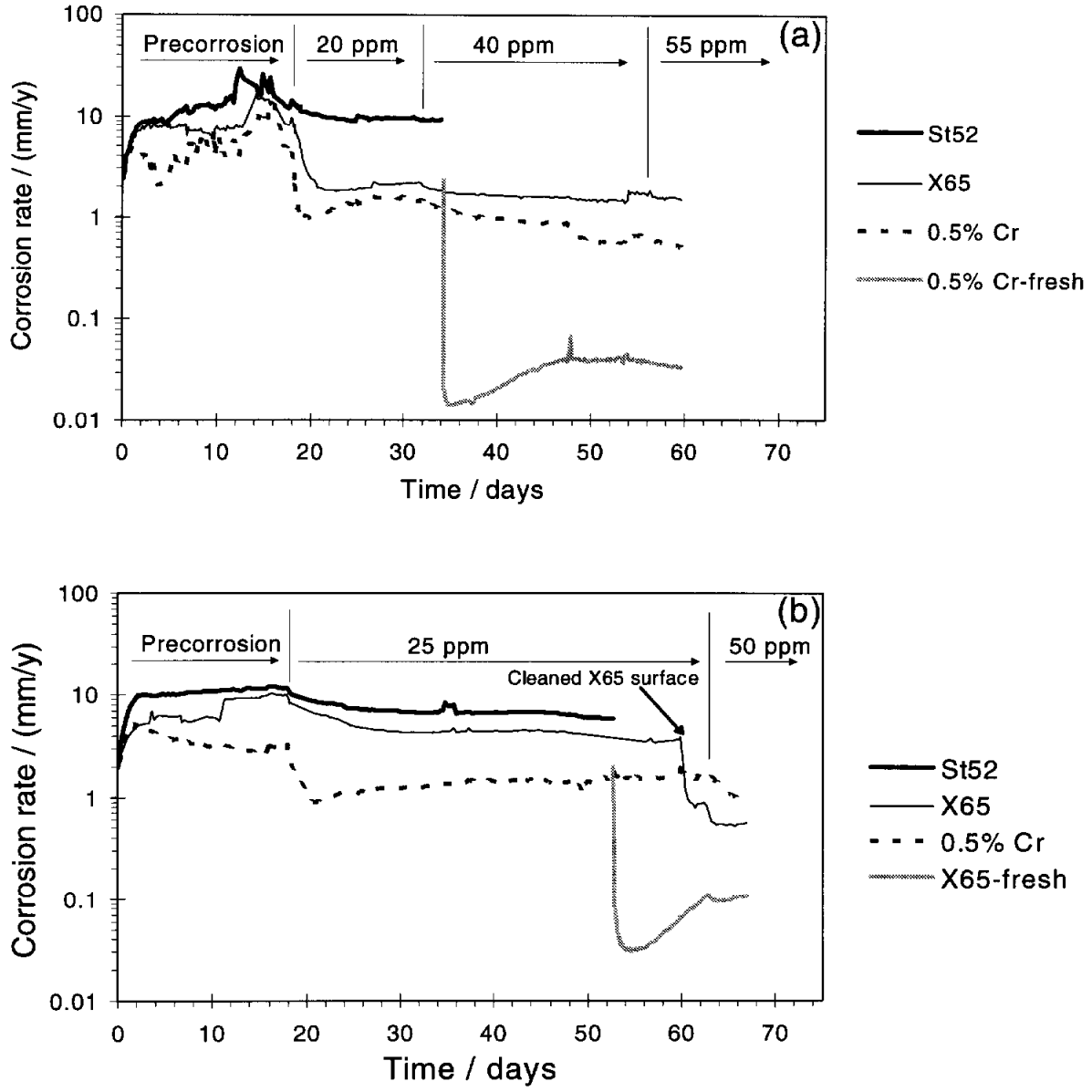

FIGURE 11. Average corrosion rate vs. time in loop experiments with (a) Inhibitor C and (b) Inhibitor D (both amine based). The inhibitor concentrations are given in the graphs. Experimental conditions: 50 °C, pH 5, 1 bar CO_2, 3 % NaCl, pipe flow 1 m/s.

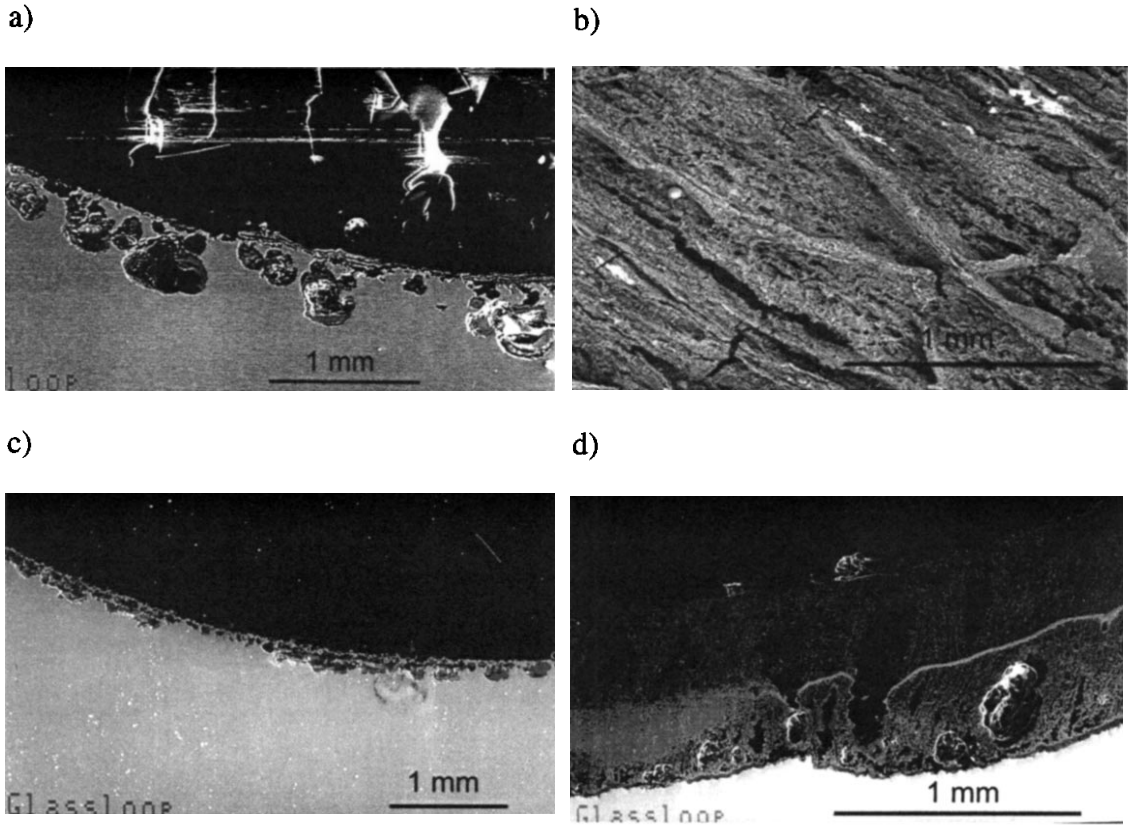

FIGURE 12. Scanning electron micrographs of specimens from the experiment in Fig. 11a. (a) cross section of X65, (b) surface image of X65, (c) cross section of 0.5 % Cr and (d) cross section of St52. Experimental condition: 50 °C, pH 5, 1 bar CO_2 , 3 % NaCl, pipe flow 1 m/s.

APPENDIX A

In Fig.4 and Fig. 10 one observes a nearly linear increase of the corrosion rate with time during precorrosion in the semi-logarithmic plots. This actually reflects an exponential increase. This can be easily explained by the positive feedback process: the cementite film increase the corrosion rate which then further increases the growth of cementite films.

The latter process can be mathematically described by writing that the growth rate of the cementite film is directly proportional to the corrosion rate (current):

$$d\delta = c_1 \, i \, dt \tag{1}$$

where δ is the thickness of the carbide film, i is the corrosion current , t is time and c_1 is the proportionality constant. For cementite lamellae (perlite) it may be assumed that the electrochemically active surface area of the cementite film increases nearly linear with the thickness of the film. The corrosion current will thus increase approximately linear with the thickness of the carbide film:

$$i = i_o + c_2 \delta \tag{2}$$

where i_o is the corrosion current on the bare metal, and c_2 is the proportionality constant. After combining the two equations one obtains:

$$di = c_3 \, i \, dt \tag{3}$$

Integrating the latter equation:

$$\int_{io}^{i} \frac{di}{i} = \int_0^{\tau} c_3 dt \tag{4}$$

gives the corrosion current as a function of time τ:

$$i = i_o \, e^{c_3 \tau} \tag{5}$$

which describes a linear increase of the corrosion rate in a semi-logaritmic plot. The slope c_3 of the best fit line for the St52 steel (0.12) in Fig. 4 is somewhat higher than for the X65 steel (0.09). This difference can be explained by the higher content of carbon in the St52 steel) which can be translated into a denser carbide film.

In order to have a galvanic coupling there must be electrically conducting paths between the cementite and the ferrite. However, the cementite is not likely to form an infinite network. Thus when the cementite film has reached a thickness comparable to the typical conducting path length, the corrosion rate should approach a steady state value, since the outer part of the film looses electrical contact with the ferrite. The St52 specimen seems to approach this condition after 14 days corrosion at 20 °C, Fig. 4. At 50 °C, however, the exponential increase in corrosion rate is completed in 2-3 days, due to the higher corrosion rate, Fig.11. After this the corrosion rate becomes more or less constant.